

Second-Order Advantage Achieved with Four-Way Fluorescence Excitation–Emission–Kinetic Data Processed by Parallel Factor Analysis and Trilinear Least-Squares. Determination of Methotrexate and Leucovorin in Human Urine

Alejandro C. Olivieri,^{*,†} Juan A. Arancibia,[†] Arsenio Muñoz de la Peña,[‡] Isabel Durán-Merás,[‡] and Anunciación Espinosa Mansilla[†]

Departamento de Química Analítica, Facultad de Ciencias Bioquímicas y Farmacéuticas, Universidad Nacional de Rosario, Suipacha 531, Rosario, S2002LRK, Argentina, and Departamento de Química Analítica, Facultad de Ciencias, Universidad de Extremadura, 06071 Badajoz, España

Four-way fluorescence data recorded by following the kinetic evolution of excitation–emission fluorescence matrices (EEMs) have been analyzed by parallel factor analysis and trilinear least-squares algorithms. These methodologies exploit the second-order advantage of the studied data, allowing analyte concentrations to be estimated even in the presence of an uncalibrated fluorescent background. They were applied to the simultaneous determination of the components of the anticancer combination of methotrexate and leucovorin in human urine samples. Both analytes were converted into highly fluorescent compounds by oxidation with potassium permanganate, and the kinetics of the reaction was continuously monitored by recording full EEM of the samples at different reaction times. A commercial fast scanning spectrofluorometer has been used for the first time to measure the four-way EEM kinetic data. The rapid scanning instrument allows the acquisition of a complete EEM in 12 s at a wavelength scanning speed of 24 000 nm/min. The emission spectra were recorded from 335 to 490 nm at 5-nm intervals, exciting from 255 to 315 nm at 6-nm intervals. Ten successive EEMs were measured at 72-s intervals, to follow the fluorescence kinetic evolution of the mixture components. Good recoveries were obtained in synthetic binary samples and also in spiked urine samples. The excitation, emission, and kinetic time profiles recovered by both chemometric techniques are in good agreement with experimental observations.

In recent years, multiway chemometric techniques have been introduced for the analysis of complex samples.¹ They are appealing to analytical chemists because they allow for a direct separation of the measured signals into the underlying contribu-

tions from individual analytes. Furthermore, instruments that easily generate multidimensional arrays of experimental data per sample are presently available to chemists. One example is a high-performance liquid chromatograph coupled to a diode array detector (HPLC-DAD).² A spectrofluorometer provides a particularly interesting possibility, because it allows, in a very straightforward manner, the acquisition of multiway information on a single instrument by recording excitation–emission matrices (EEMs).³ Both HPLC-DAD and EEM data are considered as second-order arrays per sample, leading to three-way arrays when data for a group of samples are joined.

Several second-order calibration methods have been recently described for EEM analysis, to resolve mixture components or to determine single components in complex samples, even in the presence of uncalibrated interferents. Bro et al. published a review on multiway spectroscopic analysis, covering the known procedures until 1995.⁴ Recent examples are the determination of polycyclic aromatic hydrocarbons,⁵ carbamate pesticides,⁶ ternary mixtures of naphthyl derivatives,⁷ triphenyltin in seawater,^{8,9} chlorophylls and pheopigments,¹⁰ verapamil in tablets,¹¹ propranolol, amiloride, and dipyridamole,¹² naproxen–salicylic acid in serum and naproxen–salicylic acid–salicylic acid in urine,¹³ norfloxacin, enoxacin, and ofloxacin fluoroquinolones in serum,¹⁴

- (2) Johnson, K.; De Juan, A.; Rutan, S. C. *J. Chemom.* **1999**, *13*, 331–341.
- (3) Andersen, C. M.; Bro, R. *J. Chemom.* **2003**, *17*, 200–215.
- (4) Bro, R.; Workman, J. J., Jr.; Mobley, P. R.; Kowalski, B. R. *Appl. Spectrosc. Rev.* **1997**, *32*, 237–261.
- (5) Beltran, J. L.; Guiteras, J.; Ferrer, R. *Anal. Chem.* **1998**, *70*, 1949–1955.
- (6) Jiji, R. D.; Booksh, K. S. *Anal. Chem.* **2000**, *72*, 718–725.
- (7) Cao, Y. Z.; Chen, Z. P.; Mo, C. Y.; Wu, H. L.; Yu, R. Q. *Analyst* **2000**, *125*, 2303–2310.
- (8) Saurina, J.; Tauler, R. *Analyst* **2000**, *125*, 2038–2043.
- (9) Saurina, J.; Leal, C.; Compañó, R.; Granados, M.; Tauler, R.; Prat, M. D. *Anal. Chim. Acta* **2000**, *409*, 237–245.
- (10) Moberg, L.; Robertson, G.; Karlberg, B. *Talanta* **2001**, *54*, 161–170.
- (11) Esteves da Silva, J. C. G.; Litao, J. M. M.; Costa, F. S.; Ribeiro, J. L. A. *Anal. Chim. Acta* **2002**, *453*, 105–115.
- (12) Cao, Y. Z.; Mo, C. Y.; Long, J. G.; Chen, H.; Wu, H. L.; Yu, R. Q. *Anal. Sci.* **2002**, 333–336.
- (13) Arancibia, J. A.; Olivieri, A. C.; Escandar, G. M. *Anal. Bioanal. Chem.* **2002**, *374*, 451–459.

* To whom correspondence should be addressed. E-mail: aolivier@bioyf.unr.edu.ar.

[†] Universidad Nacional de Rosario.

[‡] Universidad de Extremadura.

(1) Faber, N. M.; Bro, R.; Hopke, P. K. *Chemom. Intell. Lab. Syst.* **2003**, *65*, 119–137.

doxorubicin in plasma,¹⁵ piroxicam in serum,¹⁶ carbendazin, fuberidazole, and thiabendazole pesticides,¹⁷ ibuprofen in pharmaceutical preparations and serum,¹⁸ carbamazepine in serum and pharmaceutical preparations,¹⁹ and ciprofloxacin in urine.²⁰ The list gives an idea of the variety of analytes and samples that are being explored within this rapidly expanding field.

The different multiway methods used to resolve multicomponent mixtures belong to three main groups: (1) direct solution, (2) iterative, and (3) least-squares methods. The first group includes the generalized rank annihilation method (GRAM)²¹ and direct trilinear decomposition (DTLD).²² Examples of iterative methods are parallel factor analysis (PARAFAC),²³ self-weighted alternating trilinear decomposition (SWATLD),²⁴ multivariate curve resolution coupled to alternating least squares (MCR-ALS)²⁵ and *N*-way partial least squares (N-PLS).²⁶ Bilinear least squares (BLLS) is a recently introduced technique, based on a direct least-squares procedure.^{27,28} Iterative algorithms have been most widely employed, as they are considered to be less sensitive to instrumental noise and model deviations. Especially useful are PARAFAC and SWATLD, particularly when the data follow the so-called trilinear model.²⁶ This is due to the fact that decomposition of a three-way data array built with response matrices measured for a number of samples is often unique, allowing spectral profiles as well as relative concentrations of individual sample components to be extracted directly. This property has been named the *second-order advantage*²⁹ and is fully exploited by both PARAFAC and SWATLD. It should be noticed that BLLS coupled to a separate procedure called residual bilinearization (RBL) has been shown to be useful in this regard.²⁰ Among all the methods listed above, N-PLS is the only one that is not able to exploit the second-order advantage, because it cannot model interferences that are not present in the training sample set.

Kinetic experiments provide the opportunity of introducing an additional temporal dimension in the measured data set, allowing one to increase the selectivity of spectroscopic-based determinations. Three-way kinetic measurements have been reported in the literature, by following the time evolution of absorption or emission spectra.^{30,31} However, only in a few cases have four-way data been recorded by measuring the time evolution of EEMs and used to

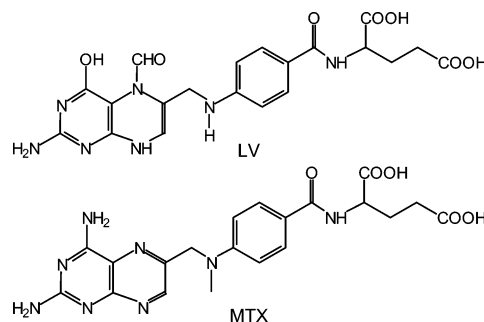


Figure 1. Chemical structures of leucovorin (LV) and methotrexate (MTX).

build quantitative calibration models. Kinetic fluorescence detection was employed by Gui et al.³² to determine glycine and glutamine after thin-layer chromatographic separation, using DTLD to analyze the resulting four-way data. Tau et al. resolved four-way data arrays by PARAFAC in a kinetic system that involved the simultaneous degradation of spinach-extracted chlorophylls a and b, initiated by treatment with an acid buffer.³³ Nikolajsen et al. described the determination of adrenaline and noradrenaline by EEM measurements of the fluorescing 3,5,6-trihydroxyindole derivatives of the catecholamines as a function of time³⁴ and used PARAFAC and N-PLS to resolve the mixture components. To acquire EEMs as a function of time, a laboratory-constructed charge-coupling device fluorometer was used, as previously described by Muroski et al.³⁵

In the present report, we analyze four-way kinetic fluorescence data for a system composed of the antineoplastic combination methotrexate/leucovorin embedded in a human urine background. This type of data should in principle exhibit the same advantage shown by three-way data as regards the presence of uncalibrated components, i.e., the second-order advantage, while providing additional selectivity. It may be noticed that Booksh and Kowalski, when referring to third-order data, suggested the term *third-order advantage*, although they stated that “the complete third-order advantage, or the *N*th-order advantage for that matter, is unknown”.²⁹ For the purpose of investigating the analytical properties of third-order data, we compare the performances of PARAFAC and a new technique, which we call trilinear least squares (TLLS), developed as an extension of BLLS for quadrilinear data and presented for the first time in this paper. Particular attention is focused on the ability of these techniques in achieving the second-order advantage. To the best of our knowledge, this is the first report on the achievement of the second-order advantage using four-way data for analytes embedded in truly complex biological samples.

Methotrexate (MTX, 2,4-diamino-*N*¹⁰-methylpteroylglutamic acid, amethopterin, Figure 1) is a prototype folate-antagonist cytotoxic drug employed in the therapy of solid tumors and leukaemias. Recently, it has also been used as an immunosuppressive agent in organ transplantation, in the treatment of some

- (14) Muñoz de la Peña, A.; Espinosa-Mansilla, A.; González-Gómez, D.; Olivieri, A. C.; Goicoechea, H. C. *Anal. Chem.* **2003**, *75*, 2640–2646.
 (15) Trevisan, M. G.; Poppi, R. J. *Anal. Chim. Acta* **2003**, *493*, 69–81.
 (16) Arancibia, J. A.; Escandar, G. M. *Talanta* **2003**, *60*, 1113–1121.
 (17) Rodríguez-Cuesta, M. J.; Boque, R.; Rius, F. X.; Picon-Zamora, D.; Martínez-Galera, M.; Garrido-Frenich, A. *Anal. Chim. Acta* **2003**, *491*, 47–56.
 (18) Hergert, L. A.; Escandar, G. M. *Talanta* **2003**, *60*, 235–246.
 (19) Escandar, G. M.; González Gómez, D.; Espinosa Mansilla, A.; Muñoz de la Peña, A.; Goicoechea, H. C. *Anal. Chim. Acta* **2004**, *506*, 161–170.
 (20) Damiani, P. C.; Nepote, A. J.; Bearzotti, M.; Olivieri, A. C. *Anal. Chem.*, in press.
 (21) Sánchez E.; Kowalski, B. R. *Anal. Chem.* **1986**, *58*, 496–499.
 (22) Sánchez E.; Kowalski, B. R. *J. Chemom.* **1988**, *2*, 265–280.
 (23) Bro, R. *Chemom. Intell. Lab. Syst.* **1997**, *38*, 149–171.
 (24) Chen, Z. P.; Wu, H. L.; Jiang, J. H.; Li, Y.; Yu, R. Q. *Chemom. Intell. Lab. Syst.* **2000**, *52*, 75–86.
 (25) Esteban, M.; Ariño, C.; Díaz-Cruz, J. N.; Díaz-Cruz, M. S.; Tauler, R. *Trends Anal. Chem.* **2000**, *19*, 49–61.
 (26) Bro, R. *J. Chemom.* **1996**, *10*, 47–61.
 (27) Linder, M.; Sundberg, R. *Chemom. Intell. Lab. Syst.* **1998**, *42*, 159–178.
 (28) Linder, M.; Sundberg, R. *J. Chemom.* **2002**, *16*, 12–27.
 (29) Booksh, K. S.; Kowalski, B. R. *Anal. Chem.* **1994**, *66*, 782A–791A.
 (30) Coello, J.; Maspocho, S.; Villegas, N. *Talanta* **2000**, *53*, 627–637.
 (31) Espinosa-Mansilla, A.; Muñoz de la Peña, A.; Goicoechea, H. C.; Olivieri, A. C. *Appl. Spectrosc.* **2004**, *58*, 83–90.

- (32) Gui, M.; Rutan, S. C.; Agbodjan, A. *Anal. Chem.* **1995**, *67*, 3293–3299.
 (33) Tan, Y.; Jiang, J. H.; Wu, H. L.; Cui, H.; Yu, R. Q. *Anal. Chim. Acta* **2000**, *412*, 195–202.
 (34) Nikolajsen, R. P. H.; Booksh, K. S.; Hansen, A. M.; Bro, R. *Anal. Chim. Acta* **2003**, *475*, 137–150.
 (35) Muroski, A. R.; Booksh, K. S.; Myrick, M. L. *Anal. Chem.* **1996**, *68*, 3534–3538.

autoimmune diseases, and in the therapy of severe asthma and rheumatoid arthritis.³⁶ The inherent risk of toxicity from high-dose therapy requires MTX monitoring in plasma or serum and the coadministration of folinic acid (LV; leucovorin, *N*⁵-formyltetrahydrofolate, Figure 1), which is used as rescue agent. High-dose methotrexate (>500 mg/m²) combined with leucovorin has been found to improve the outcome in acute lymphatic leukemia, lymphoma, and osteosarcoma.³⁷

MTX is present in several biological samples, such as plasma, serum, urine, or saliva, and can be extracted, separated, and detected under a variety of chromatographic conditions. Few papers have reported fluorescence methodologies for analyzing these compounds, because most studies are guided by HPLC. Rubino published a review where more than 70 papers describing chromatographic assays for MTX and its metabolites are discussed,³⁸ some of which involve fluorescence detection. On the other hand, the use of HPLC for the determination of folates is well documented: there are several liquid chromatography methods for the determination of LV in mixed folates and antifolates by a combination of UV and fluorometric detection.^{39–41}

The simultaneous determination of both MTX and LV presents several difficulties.^{39,40} HPLC using on-line postcolumn UV irradiation and fluorescence detection,⁴⁰ capillary electrophoresis,⁴² and net analyte-based multivariate calibration of spectrophotometric data (developed in our laboratory)⁴³ have been proposed for this purpose. Interestingly, both analytes can be transformed into highly fluorescent derivatives by reaction with hydrogen peroxide or potassium permanganate. The fluorescence properties of the products generated by the latter reagent have been established, and two separate kinetic–fluorometric methods have been previously proposed, based on analyte oxidation at different pH values.^{44,45} These kinetic reactions, previously investigated in our laboratory, form the basis of the present methodology for generating four-way data, which are adequate for the simultaneous determination of methotrexate and leucovorin in urine samples. The kinetics of the permanganate reaction was followed by measuring the EEM evolution with time, using for the first time a fast-scanning commercial spectrofluorometer, and both PARAFAC and TLLS models were applied to resolve the mixtures.

EXPERIMENTAL SECTION

Apparatus. Fluorescence spectral measurements were performed on a Varian Cary Eclipse fluorescence spectrophotometer, equipped with two Czerny–Turner monochromators and a xenon

flash lamp. The fluorometer was connected to a PC microcomputer via an IEEE 488 (GPIB) serial interface. The Cary Eclipse software was used for data acquisition, data interpretation, and graphical display. Excitation–emission matrices were recorded in a 10-mm quartz cell at 30 °C, by use of a thermostatic cell holder and a Selecta thermostatic bath. The instrument is able to scan at 24,000 nm/min without peak shifts due to the design of the monochromator drive mechanism. The grating is moved only when the lamp is off, resulting in a go-to-flash method of taking a measurement. The wavelength does not change while measurements are being made. According to the manufacturer specifications of the instrument, the wavelength accuracy is ±1.5 nm and the wavelength reproducibility is ±0.2 nm.

Reagents. All experiments were performed with analytical reagent grade chemicals. LV (as the calcium salt pentahydrate) was prepared by dissolving 0.0100 g of reagent (Acros Organics) in 100 mL of ultrapure water obtained using Water Pro PS equipment (Labconco, Kansas City, MO). MTX was prepared by dissolving 0.0100 g of the compound (Sigma, St. Louis, MO) in 100 mL of alkalized ultrapure-grade water. Appropriate MTX and LV solutions of different concentrations were prepared by dilution in ultrapure-grade water. A 0.1000 M KMnO₄ stock solution (standardized by titration with sodium oxalate) was prepared in doubly distilled water. A Borax 0.065 M buffer of pH 9.4 was also used.

Calibration and Test Sets. In this work, the method of external calibration was employed. For this purpose, a calibration set of nine samples was constructed, using a central composite design with five levels of MTX and LV. The levels correspond to values in the range 0.00–0.98 mg L⁻¹ for MTX and 0.00–0.68 mg L⁻¹ for LV. The procedure consisted in placing an aliquot of 3 mL of each solution containing adequate quantities of both MTX and LV and Borax buffer of pH 9.4 in the quartz cell, adding 50 μL of 0.028 M KMnO₄, and mixing. The kinetic evolution of excitation–emission fluorescence matrices of these solutions was then recorded, and the obtained data were subjected to four-way analysis, as described below.

In principle, exploratory excitation and emission wavelength ranges were 240–350 nm for excitation and 330–520 nm for emission, but in order to avoid the presence of Rayleigh scattering and diffraction grating harmonics, the EEMs were then recorded in restricted ranges. The latter were as follows: emission from 335 to 490 nm at 5-nm intervals (*J* = 32 data points) and excitation from 255 to 315 nm at 6-nm intervals (*K* = 11 data points), making a total of 352 spectral points per sample matrix. The rapid-scanning instrument allows the acquisition of a complete EEM in 12 s at a wavelength scanning speed of 24 000 nm/min. In the time dimension, the EEMs were obtained at intervals of 72 s, for a reaction time ranging from 0 to 10.8 min. Since 10 data points were collected in the latter mode, each three-way array consisted of a total of 3520 data points. It should be noticed that, if reaction significantly evolves during spectral acquisition, the data sample would not be strictly trilinear. In our case, we did not find this problem to be important. However, we have to note that the proposed approach, using total EEM spectra acquisition, will not be appropriated, in general, for fast kinetic studies.

The binary test set was composed of 10 samples, prepared in the same form as those for calibration, but using a random design,

- (36) Parfitt, K.; Sweetman, S. C.; Blake, P. S.; Parsons, A. V. *The Extra Pharmacopeia*, 32th ed.; Pharmaceutical Press: London, 1999; pp 547–541.
- (37) Graf, N.; Winkler, K.; Betlemovic, M.; Fuchs, N.; Bode, U. *J. Clin. Oncol.* **1994**, *12*, 1443–1451.
- (38) Rubino, F. M. *J. Chromatogr., B* **2001**, *764*, 217–254.
- (39) Belz, S.; Frickel, C.; Wolfrom, C.; Nau, H.; Henze, G. *J. Chromatogr., B* **1994**, *661*, 109–118.
- (40) Mandl, A.; Linder, W. *Chromatographia* **1996**, *43*, 327–330.
- (41) Duan, G. L.; Zheng, L. X.; Chen, J.; Cheng, W. B.; Li, D. *Biomed. Chromatogr.* **2002**, *16*, 282–286.
- (42) Sczesny, F.; Hempel, G.; Boos, J.; Blaschke, G. *J. Chromatogr., B: Biomed. Appl.* **1998**, *718*, 177–185.
- (43) Espinosa Mansilla, A.; Durán Merás, I.; Rodríguez Gómez, M. J.; Muñoz de la Peña, A.; Salinas, F. *Talanta* **2002**, *58*, 255–263.
- (44) Durán Merás, I.; Espinosa Mansilla, A.; Rodríguez Gómez, M. J.; Salinas, F. *Talanta* **2001**, *55*, 623–630.
- (45) Espinosa Mansilla, A.; Durán Merás, I.; Zamoro Madera, A.; Pedano, L.; Ferreyra, C. *J. Pharm. Biomed. Anal.* **2002**, *29*, 851–858.

i.e., selecting the target concentrations of both analytes at random from the calibration range for each analyte (see below for details on the composition of these samples).

Urine Samples. Volumes of 40 μL of six different urine samples (taken from different healthy individuals), also containing 2 mL of Borax buffer of pH 9.4, were spiked with concentrations of both analytes, selected at random from their corresponding calibration ranges, and diluted to 10.00 mL with water in volumetric flasks. Then 3 mL of these solutions were placed in the quartz cell and treated with potassium permanganate as described for the calibration and test set. Three additional urine samples were treated in the same manner but were left as blanks; i.e., they were not spiked with the analytes. The evolutions of the EEMs with time were subsequently read for all these samples in the same manner as described above. Each urine sample was prepared in duplicate (details on the nominal analyte concentrations for these samples are provided below). The level of urine dilution (1:250) implies that the present calibration scheme covers concentration ranges up to 245 mg L^{-1} for MTX and 170 mg L^{-1} for LV, values which are comparable to those found in patients.

38,46

THEORY

PARAFAC. A given sample produces third-order data when a $J \times K \times L$ data array (or third-order array) is experimentally obtained, where J , K , and L denote the number of data points in each of the three dimensions (in kinetic–EEM fluorescence measurements, J is the number of digitized emission wavelengths, K is the number of excitation wavelengths, and L is the number of time data points). One way of analyzing this type of data is to join the I training arrays $\mathbf{X}_{i,\text{cal}}$ and the unknown sample array \mathbf{X}_u into a four-way data array \mathbf{X} , whose dimensions are $[(I + 1) \times J \times K \times L]$. Provided \mathbf{X} follows a multilinear PARAFAC model, it can be mathematically written in terms of four vectors for each responsive component. These are designated as \mathbf{a}_n , \mathbf{b}_n , \mathbf{c}_n , and \mathbf{d}_n and collect the relative concentrations $[(I + 1) \times 1]$, emission profiles ($J \times 1$), excitation profiles ($K \times 1$), and time profiles ($L \times 1$) for component n , respectively. The specific expression is thus⁴⁷

$$X_{ijkl} = \sum_{n=1}^N a_{in} b_{jn} c_{kn} d_{ln} + E_{ijkl} \quad (1)$$

where N is the total number of responsive components, a_{in} is the relative concentration of component n in the i th sample, and b_{jn} , c_{kn} , and d_{ln} are the normalized intensities at the emission wavelength j , excitation wavelength k , and time l , respectively. The values of E_{ijkl} are the elements of the array \mathbf{E} , which is a residual error term of the same dimensions as \mathbf{X} . The column vectors \mathbf{a}_n , \mathbf{b}_n , \mathbf{c}_n , and \mathbf{d}_n are collected into the corresponding loading matrices \mathbf{A} , \mathbf{B} , \mathbf{C} , and \mathbf{D} (\mathbf{b}_n , \mathbf{c}_n , and \mathbf{d}_n are usually normalized to unit length).

The model described by eq 1 defines a decomposition of \mathbf{X} , which provides access to spectral profiles (\mathbf{B} and \mathbf{C}), time profiles (\mathbf{D}), and relative concentrations (\mathbf{A}) of individual components in

the $(I + 1)$ mixtures, whether they are chemically known or not. This constitutes the basis of the second-order advantage. The decomposition is usually accomplished through an alternating least-squares (ALS) minimization scheme.^{23,48} It should be noted that kinetic–spectral data of the type presently discussed may present the phenomenon of *rank deficiency*, meaning that the data rank is smaller than the number of the intervening chemical species. In these cases, it is sometimes preferable to apply nonnegativity constraints in PARAFAC modes during the least-squares minimization.³¹ In the present analytical problem, however, two basically nonfluorescent analytes occur that develop intense fluorescence upon oxidation, while urine is degraded to nonfluorescent products with time. Therefore, there is no rank deficiency, because a single fluorescent species occurs for each chemical reaction. As expected, calculations run by imposing nonnegativity to PARAFAC do not significantly change the prediction results.

Issues relevant to the application of the PARAFAC model to four-way kinetic–fluorescent data are as follows: (1) establishing the number of fluorophores and the reliability of the model, (2) identifying specific fluorescent components from the information provided by the model, and (3) calibrating the model in order to obtain absolute concentrations for a particular component in an unknown sample.

The number of responsive components (N) can be estimated by several methods. A useful technique is the consideration of the PARAFAC internal parameter known as core consistency (see below).⁴⁹ A PARAFAC model constructed with the correct number of components is considered to be correct if reasonably low least-squares errors are obtained in comparison with the instrumental noise level.

Identification of the chemical constituent under investigation is done with the aid of the spectral and time profiles, as extracted by PARAFAC, and comparing them with those for a standard solution of the analyte of interest. This is required since the components obtained by decomposition of \mathbf{X} are sorted according to their contribution to the overall spectral variance, and this order is not necessarily maintained when the unknown sample is changed.

Absolute analyte concentrations are obtained after calibration, because the four-way array decomposition only provides relative values (\mathbf{A}). Calibration is done by means of the set of standards with known analyte concentrations (contained in an $I \times 1$ vector \mathbf{y}) and regression of the first I elements of column \mathbf{a}_n against \mathbf{y} :

$$k = \mathbf{y}^+ \times [a_{1n}] \dots [a_{In}] \quad (2)$$

where “+” implies taking the pseudoinverse. Conversion of relative to absolute concentration of n in the unknown proceeds by division of the last element of column \mathbf{a}_n [$a_{(I+1)n}$] by the slope of the calibration graph k :

$$y_u = a_{(I+1)n} / k \quad (3)$$

In summary, the PARAFAC model first joins the I calibration data matrices together with the unknown sample matrix and then introduces concentration information in a separate pseudounivariate regression step.

(46) Crom, W. R.; Evans, W. E. Methotrexate. In *Applied pharmacokinetics. Principles of therapeutic drug monitoring*; Evans, W. E., Schentag, J. J., Jusko, W. J., Eds.; Applied Therapeutics: Vancouver, WA, 1992.

(47) Leurgans, S.; Ross, R. T. *Stat. Sci.* **1992**, *7*, 289–319.

TLLS. TLLS can be regarded as an extension of BLLS, whose formulation is discussed in detail in the relevant literature.^{27,28} As in the case of PARAFAC, a training set is required composed of I mixtures of the N_{cal} analytes (see below). However, in contrast to PARAFAC, analyte concentration information is introduced in the training step, without including data for the unknown sample. As in BLLS, the trilinear extension TLLS assumes that the data follow a trilinear structure and that the contribution of each analyte to the overall signal is given by the product of a unit-concentration pure analyte array $\underline{\mathbf{S}}_n$ (of size $J \times K \times L$) by its concentration. The least-squares TLLS model is best understood in terms of vectorized arrays, as shown in eq 4,⁵⁰ where $\text{vec}(\cdot)$ indicates the

$$[\text{vec}(\underline{\mathbf{X}}_{1,\text{cal}}) | \text{vec}(\underline{\mathbf{X}}_{2,\text{cal}}) | \dots | \text{vec}(\underline{\mathbf{X}}_{I,\text{cal}})] = [\text{vec}(\underline{\mathbf{S}}_1) | \text{vec}(\underline{\mathbf{S}}_2) | \dots | \text{vec}(\underline{\mathbf{S}}_{N_{\text{cal}}})] \mathbf{Y}^T + \mathbf{E} \quad (4)$$

vectorization operator, \mathbf{Y} is an $I \times N_{\text{cal}}$ matrix containing the concentrations of the N_{cal} calibrated analytes in the I mixtures, and \mathbf{E} is a residual term of appropriate dimensions ($JKL \times I$). To obtain least-squares approximations to the pure analyte three-way arrays at unit concentration $\underline{\mathbf{S}}_n$, a procedure analogous to the estimation of unit-concentration pure analyte spectra in first-order classical least-squares analysis is applied. The concentration product matrix \mathbf{D} (size $N_{\text{cal}} \times N_{\text{cal}}$) and N_{cal} concentration-weighted $\underline{\mathbf{T}}_n$ three-way arrays (size $J \times K \times L$) are first obtained, starting from the matrix \mathbf{Y} and the I training three-way $\underline{\mathbf{X}}_{i,\text{cal}}$ arrays:

$$\underline{\mathbf{T}} = \sum_{i=1}^I Y_{in} \underline{\mathbf{X}}_{i,\text{cal}} \quad (5)$$

$$\mathbf{D} = \mathbf{Y}^T \mathbf{Y} \quad (6)$$

Analogously to BLLS, the $\underline{\mathbf{S}}_n$ arrays are then given by

$$\underline{\mathbf{S}}_n = \sum_{i'=1}^{N_{\text{cal}}} (D^{-1})_{ni'} \underline{\mathbf{T}}_{i'} \quad (7)$$

Notice that the \mathbf{Y} matrix in TLLS contains all calibrated analytes, in our case MTX and LV. The latter should be present in the training samples in either their pure forms or as mixtures; the latter possibility is usually better and follows a proper statistical design. It is also possible to have training samples that contain mixtures of the analytes with other constituents, as long as the analyst knows the concentrations of the analytes of interest in the training samples. In this sense, the requirements for designing \mathbf{Y} are the same as those for PARAFAC.

The obtained $J \times K \times L$ arrays $\underline{\mathbf{S}}_n$ allow one to estimate the calibrated three-mode profiles for the calibrated analytes. The procedure already discussed for BLLS, and known as SVD profile estimation (SVD implies singular value decomposition) can be extended one further dimension by constructing a single-component Tucker3 model for each $\underline{\mathbf{S}}_n$ ^{27,28} which is analogous to

a single-component three-way PARAFAC model for each $\underline{\mathbf{S}}_n$:

$$S_{n,jkl} = g_n b_{jn} c_{kn} d_{ln} + E_{n,jkl} \quad (8)$$

where $S_{n,jkl}$ is a (j,k,l) element of $\underline{\mathbf{S}}_n$, g_n is the normalization core, b_{jn} , c_{kn} and d_{ln} are elements of \mathbf{b}_n , \mathbf{c}_n , and \mathbf{d}_n , the emission ($J \times 1$), excitation ($K \times 1$), and time ($L \times 1$) profiles for component n , respectively, and $E_{n,jkl}$ is an element of the residual term $\underline{\mathbf{E}}_n$ (of the same dimensions as $\underline{\mathbf{S}}_n$). The profiles provided by eq 8 should be similar to those described above for PARAFAC (notice, however, that they do not include uncalibrated components, which may occur in the unknown sample). One difference with PARAFAC is that TLLS does not require the identification of calibrated components, an operation that is automatically performed by the algorithm.

If the calibration model is exact, the pure analyte arrays $\underline{\mathbf{S}}_n$ allow one to estimate the analyte concentrations in the unknown. As previously shown,⁵⁰ BLLS employs a prediction equation which is equivalent to that derived in first-order classical least-squares analysis, except that data for the pure analytes and for the unknown sample are vectorized. Analogously to BLLS, therefore, a pure analyte matrix \mathbf{S}_{cal} (of dimensions $JKL \times N_{\text{cal}}$) can be defined in TLLS by

$$\mathbf{S}_{\text{cal}} = [g_1 (\mathbf{d}_1 \otimes \mathbf{c}_1 \otimes \mathbf{b}_1) | g_2 (\mathbf{d}_2 \otimes \mathbf{c}_2 \otimes \mathbf{b}_2) | \dots | (g_{N_{\text{cal}}} \mathbf{d}_{N_{\text{cal}}} \otimes \mathbf{c}_{N_{\text{cal}}} \otimes \mathbf{b}_{N_{\text{cal}}})] \quad (9)$$

where \otimes implies the well-known Kronecker product.

The concentration of analytes in the unknown sample is then simply predicted as

$$\mathbf{y}_u = \mathbf{S}_{\text{cal}}^+ \text{vec}(\underline{\mathbf{X}}_u) \quad (10)$$

where \mathbf{y}_u is a vector (size $N_{\text{cal}} \times 1$) containing the predicted concentrations of the N_{cal} analytes in the test sample.

Uncalibrated compounds occurring in an unknown sample are analyzed by comparing the residuals of the prediction least-squares fit with the instrumental noise level (assessed by blank replication instrumental measurements). If additional components than those calibrated are required by the unknown sample, a separate iterative procedure called residual trilinearization (RTL), analogous to RBL,^{27,28} can be carried out. The latter is summarized in the following steps:

(1) Set $N_{\text{int}} = 1$ as a trial number of interfering components occurring in the unknown sample.

(2) Calculate an expanded version of \mathbf{y}_u with eq 11 and the positive residuals for the prediction step with eq 12 (the first time this RTL procedure is used, consider $\mathbf{S}_{\text{exp}} = \mathbf{S}_{\text{cal}}$, in which case \mathbf{y}_u only predicts the calibrated analytes)

$$\mathbf{y}_u = \mathbf{S}_{\text{exp}}^+ \text{vec}(\underline{\mathbf{X}}_u) \quad (11)$$

$$\underline{\mathbf{E}}_u = |\underline{\mathbf{X}}_u - \sum_{i'=1}^{N_{\text{cal}}} \underline{\mathbf{S}}_{i'} Y_{i',u}| \quad (12)$$

where \mathbf{S}_{exp} is an expanded version of \mathbf{S}_{cal} (see eq 9), which includes the interference profiles.

(48) Paatero, P. *Chemom. Intell. Lab. Syst.* **1997**, *38*, 223–242.

(49) Bro, R. Multi-way analysis in the food industry. Doctoral Thesis, University of Amsterdam, Amsterdam, The Netherlands, 1998.

(50) Faber, N. M.; Ferré, J.; Boqué, R.; Kalivas, J. H. *Chemom. Intell. Lab. Syst.* **2002**, *63*, 107–116.

(3) Build a Tucker3 model with N_{int} components in each of the three modes for the three-way array $\underline{\mathbf{E}}_u$ and obtain the profiles for the interference(s),

$$(\mathbf{A}_{\text{int}} \otimes \mathbf{B}_{\text{int}} \otimes \mathbf{C}_{\text{int}} \otimes \mathbf{D}_{\text{int}}) = \text{Tucker3}(\underline{\mathbf{E}}_u) \quad (13)$$

where \mathbf{A}_{int} is the core array.

(4) Expand \mathbf{S}_{cal} by including the interference profiles.

(5) Return to step 2 and continue until convergence.

(6) If the residuals are still significantly larger than the noise level, return to step 1 and increase the number of interferences by one. Notice that the final value of N in TLLS is given by $N_{\text{cal}} + N_{\text{int}}$.

As can be seen, the TLLS philosophy involves a two-step calibration–prediction mode. The second-order advantage is left for a postcalibration stage, in which the residuals are trilinearized for estimating interference profiles. The latter are useful for correctly estimating the analyte concentrations, even in the presence of unexpected constituents.

Figures of Merit. Figures of merit are analytical parameters used for the comparison of methods. Different approaches have been discussed in the literature for computing figures of merit for higher order methodologies.^{51–54}

As regards the sensitivity, the following equation seems to apply to the presently studied case:^{53,55,56}

$$\text{SEN} = k \{ [[(\mathbf{B}^T \mathbf{B}) * (\mathbf{C}^T \mathbf{C}) * (\mathbf{D}^T \mathbf{D})]^{-1}]_{nn} \}^{-1/2} \quad (14)$$

where “*” is the element-wise product operator and k is an appropriate scaling factor. In PARAFAC, k is identified with the proportionality constant between scores and concentrations (eq 2), while in TLLS it can be obtained by regressing the g_n values (eq 8) against \mathbf{y} . Note that when urine is included in the samples, \mathbf{B} , \mathbf{C} , and \mathbf{D} include interference profiles and hence a decrease in sensitivity is expected. When the second-order advantage is achieved, eq 14 implies a SEN value that is sample-specific and that cannot be defined for the multivariate method as a whole. We thus report average values for a set of representative samples.

A further figure of merit is the standard error in the predicted concentrations, an area of active research in the multivariate calibration field. Mathematical expressions for sample-specific prediction uncertainties take proper account of the propagation of different error sources but are unavailable for cases exploiting the second-order advantage.⁵⁷ A useful alternative is to resort to mean prediction errors for a set of test samples, to obtain an average concentration error, useful for method comparison (see below).

The limit of detection (LOD) has been recently discussed for higher-order multivariate techniques by means of a rigorous

approach that considers the presence of both false positive and false negative errors.^{58,59} A recent work has discussed the estimation of the PARAFAC LOD, but only when all sample components present are calibrated.⁵⁷ This latter approach is therefore not applicable to the analyte determination in urine samples. The LOD can still be estimated using the expression⁵⁷

$$\text{LOD} = 3s_r/\text{SEN} \quad (15)$$

where s_r is the instrumental noise level and the appropriate SEN value is employed. Equation 15 does not account for calibration uncertainties, and hence, it generally provides overoptimistic values. In the case of urine samples, because the value of SEN is given as an average value over a test sample set, LOD is also reported as an average figure.

Software. All calculations were done using MATLAB 6.0,⁶⁰ using the PARAFAC routines developed by Bro and available on the Internet.⁶¹ We have developed a MATLAB graphical interface, similar to that already described for first-order multivariate calibration.⁶² It implements PARAFAC and also TLLS and offers a simple graphical means in which data can be loaded into the working space, spectral and time regions can be selected, and three-mode profiles and pseudounivariate calibration graphs can be plotted. Analytically relevant results, i.e., predicted concentration and figures of merit, are conveniently shown.

RESULTS AND DISCUSSION

Kinetic Behavior of the Analytes. In previous papers,^{44,45} the oxidation reactions of MTX and LV in the presence of potassium permanganate were described. The oxidation of MTX takes place in acid media (pH at ~ 5), while LV is readily oxidized in strongly alkaline solutions (0.17 M NaOH). In the present paper, we selected a pH value (9.4) where the oxidation of both analytes occurs at measurable rates. Under these conditions, kinetic excitation–emission matrices have been recorded that contain relevant information concerning the fluorescent reaction products of both MTX and LV.

On the other hand, urine is a complex biological mixture exhibiting strong native fluorescence and whose behavior under the presently studied oxidizing conditions was not known in advance. Our results suggest that the main phenomenon occurring when a diluted urine sample is subjected to alkaline oxidation with permanganate is a decrease in the initial fluorescence emission, with a time scale comparable to those of the analytes. This allowed us to probe the success of the different chemometric approaches in recovering not only the fluorescence spectral profiles of the different sample components but also the corresponding behaviors as time evolves.

Spectral Properties of Analytes. Figure 2 shows the superimposed contour plots corresponding to the EEM for one of the training samples (containing MTX 0.39 mg L⁻¹ and LV 0.38 mg

(51) Messick, N. J.; Kalivas J. H.; Lang, P. M. *Anal. Chem.* **1996**, *68*, 1572–1579.

(52) Wang, Y.; Borgen, O. S.; Kowalski, B. R.; Gu M.; Turecek, F. *J. Chemom.* **1993**, *7*, 117–130.

(53) Faber, K.; Lorber, A.; Kowalski B. R. *J. Chemom.* **1997**, *11*, 419–461.

(54) Ho, C.-N.; Christian G. D.; Davidson, E. R. *Anal. Chem.* **1980**, *52*, 1071–1079.

(55) Faber, N. M. *J. Chemom.* **2001**, *15*, 743–748.

(56) Olivieri, A. C. *J. Chemom.*, submitted for publication.

(57) Olivieri, A. C.; Faber, N. M. *Chemom. Intell. Lab. Syst.* **2004**, *70*, 75–82.

(58) Boqué, R.; Larrechi, M. S.; Rius, F. X. *Chemom. Intell. Lab. Syst.* **1999**, *45*, 397–408.

(59) Boqué, R.; Ferré, J.; Faber, N. M.; Rius, F. X. *Anal. Chim. Acta* **2002**, *451*, 313–321.

(60) MATLAB 6.0, The MathWorks Inc., Natick, MA, 2000.

(61) <http://www.models.kvl.dk/source/>.

(62) Goicoechea, H. C.; Iñon, F. A.; Olivieri, A. C. *Chemom. Intell. Lab. Syst.*, in press.

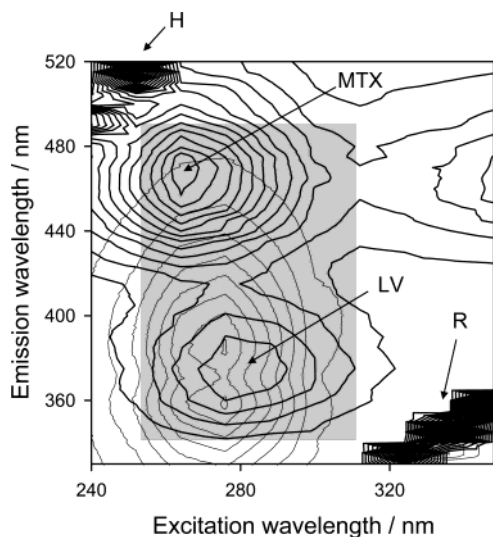


Figure 2. Contour plot of the EEM for an aqueous solution (pH 9.4) containing methotrexate 0.39 mg L^{-1} and leucovorin 0.38 mg L^{-1} (thick lines, analyte maximums are indicated for MTX and LV, respectively) and a typical human urine sample diluted 1:250 (narrow lines), showing the presence of a diffraction grating harmonics (H) and Rayleigh (R) scatterings, as indicated. The gray rectangle illustrates the spectral excitation and emission ranges selected for calibration with PARAFAC and TLLS.

L^{-1}) and for a typical human urine, in all cases after reaction with potassium permanganate at a reaction time of 4.8 min. They were recorded in wide spectral excitation and emission ranges, 240–350 and 330–520 nm, respectively, and show Rayleigh scattering and a second harmonic from the diffraction grating (Figure 2). These latter signals are undesired because they are not correlated with the target concentrations of the studied analytes. Therefore, for calibration and prediction purposes, the EEMs were subsequently recorded, as a function of time, in the sensibly restricted excitation and emission ranges shown as a gray rectangle in Figure 2, which includes the analytes' fluorescence peaks of highest intensity. This range corresponds to emission from 335 to 490 nm at 5-nm intervals ($J = 32$ data points) and excitation from 255 to 315 nm at 6-nm intervals ($K = 11$ data points), making a total of 352 spectral points per sample matrix. Figure 2 also highlights the fact that a significant overlapping occurs between the analytes and the urine background of this particular sample across the examined spectral ranges. Furthermore, the absolute intensity of urine components is, on the average, comparable to those stemming from the analytes in the investigated concentration ranges. It should also be noted that the intensity and spectral shapes of urine vary among different individuals, making it difficult to employ first-order multivariate techniques for MTX and LV monitoring, because they are sensitive to unmodeled components.

Figure 3 shows the four-way data array structure used in this work, following the time evolution of the EEM of one of the calibration mixtures in the selected spectral ranges and in the presence of potassium permanganate. It can be appreciated that the fluorescence intensity of the analytes increases considerably as a function of reaction time. This provides a sensitivity for the determination which is significantly larger than that achieved in the absence of oxidant. Furthermore, the emission intensity of urine fluorescent components decreases with time (see below),

Table 1. Predicted Concentrations in a Binary Test Set of Samples, Using Both PARAFAC and TLLS

LV/ mg L^{-1}			MTX/ mg L^{-1}		
nominal	PARAFAC	TLLS	nominal	PARAFAC	TLLS
0.25	0.27	0.28	0.60	0.46	0.48
0.44	0.44	0.47	0.18	0.14	0.09
0.14	0.09	0.14	0.14	0.01	0.08
0.51	0.53	0.51	0.74	0.65	0.59
0.31	0.30	0.31	0.49	0.38	0.39
0.38	0.34	0.38	0.05	0.03	0.01
0.17	0.12	0.18	0.00	-0.05	-0.04
0.55	0.50	0.55	0.00	0.04	-0.03
0.00	-0.02	0.00	0.39	0.20	0.33
0.27	0.24	0.25	0.40	0.37	0.40

figures of merit ^a	LV		MTX	
	PARAFAC	TLLS	PARAFAC	TLLS
RMSEP/ mg L^{-1}	0.03	0.02	0.10	0.08
SEN/ $\text{AFU } 1 \text{ mg}^{-1}$	8×10^3	8×10^3	1×10^4	1×10^4
LOD/ mg L^{-1}	0.01	0.01	0.01	0.01

^a RMSEP, root-mean-square error of prediction. AFU, arbitrary fluorescence units. The value of SEN was computed using eq 14.

providing additional selectivity when this complex biological fluid is analyzed.

Binary MTX/LV Samples. The set of 10 test binary samples was investigated with the aid of PARAFAC. Initialization was performed using the default PARAFAC option (which employs SVD vectors), and an unconstrained least-squares fit was then carried out. Although in principle two fluorophores are expected for these samples, the selection of the number of spectral components has been independently checked by the method known as core consistency diagnostic,⁶³ especially useful for spiked urine samples (see below). It is based on examining the model based on the data and the estimated parameters of gradually augmented models. The model is called appropriate if adding other combinations of the same components does not improve the fit considerably. When the core consistency drops from a high value, above $\sim 60\%$, to a low value, this indicates that an appropriately number of components has been attained. For PARAFAC, in all cases the core consistency dropped to a very low value when using three spectral components to model the data, suggesting that $N = 2$ is a sensible choice, as expected from the composition of these samples. The PARAFAC emission, excitation, and time profiles of the two-component model match those expected for pure analyte standards. In all cases, the residual least-squares errors were comparable to the instrumental noise, indicating a good fit to the proposed model.

When TLLS was applied to the same set, the study of the prediction residuals led to the conclusion that two components were sufficient to obtain a good least-squares fit for all unknown samples. In this set of binary samples, achieving reasonably low residuals implies that components additional to those considered during calibration are not necessary. The TLLS profiles for the

(63) Bro, R.; Kiers, H. A. L. *J. Chemom.* **2003**, *17*, 274–286.

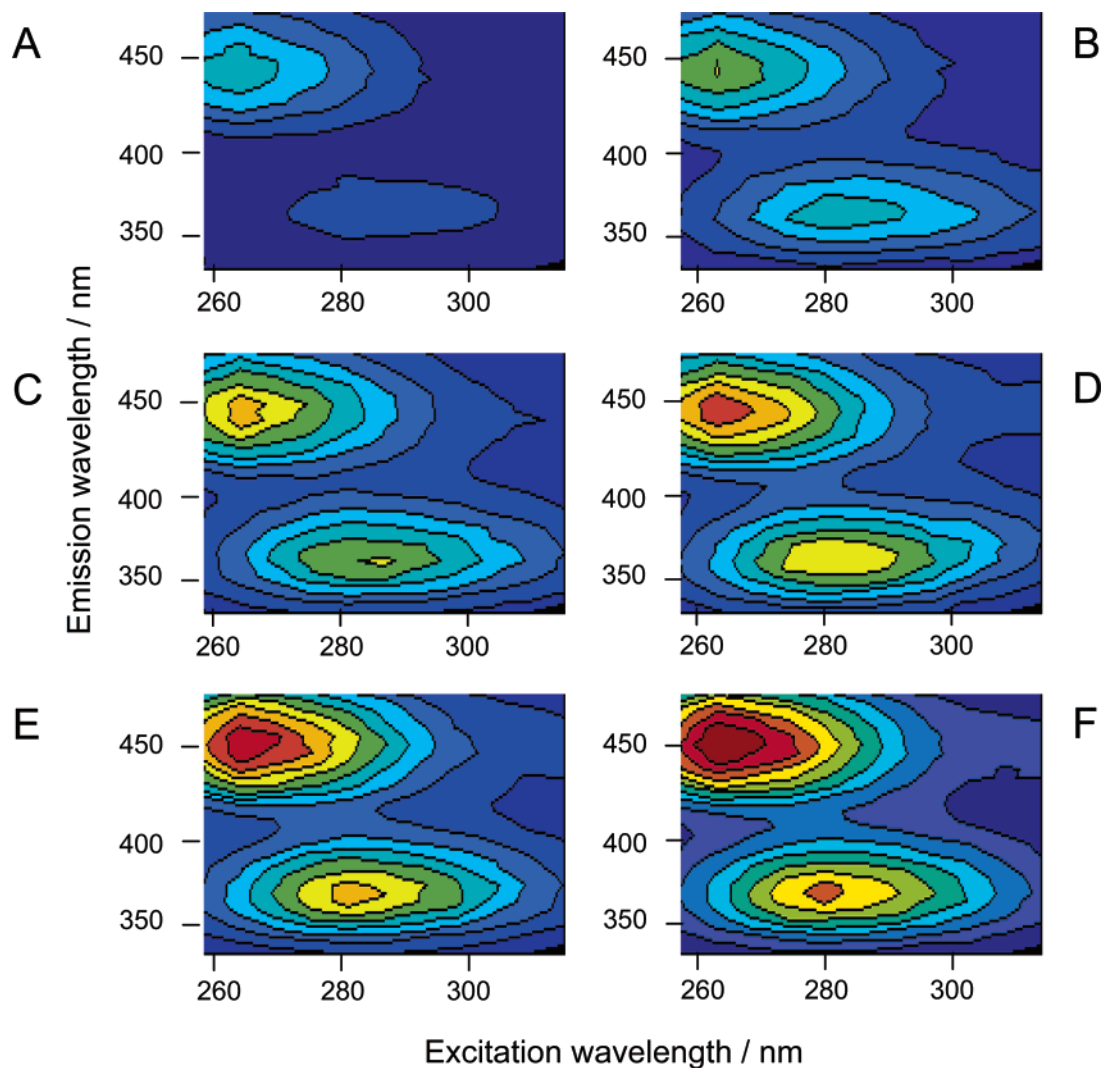


Figure 3. Contour plots of the EEMs for an aqueous solution (pH 9.4) containing methotrexate 0.68 mg L^{-1} and leucovorin 0.49 mg L^{-1} as a function of the time of permanganate oxidation. Times selected for illustrating the kinetic evolution of the EEMs (in min): (A) 0, (B) 2.4, (C) 4.8, (D) 7.2, (E) 9.6, and (F) 10.8. Fluorescence intensity has been coded in colors, with deep blue indicating the lowest value and deep red the largest one.

three modes were found to be comparable to those found by PARAFAC (see below for a full comparison in the presence of urine background).

Prediction results for the binary test set are presented in Table 1. All predictions and figures of merit are seen to be good, indicating that the present methodology may constitute the basis for a simultaneous determination of the presently studied analytes in the absence of serious interferences, for example, in pharmaceutical quality control. However, the most interesting results concern the achievement of the second-order advantage, to be applied to complex biological samples such as urine, where uncalibrated components occur.

Spiked Urine Samples. The set of urine samples (six of them spiked with both analytes and three blanks) was first investigated with the aid of PARAFAC. In this case, core consistency analysis was applied for each newly analyzed sample, since there is no guarantee that each unknown urine sample will behave in the same manner as the previously studied ones. The result was that all urine samples required the consideration of three fluorophores (see Figure 4 for the analysis of the first test sample in Table 2):

two for the analytes and the remaining one for the urine background. The fact that urine is modeled in all cases with a single component by the algorithm implies the presence of a major fluorescent component in this biological fluid, which dominates the urine background as well as the fluorescence time decay. Increasing the number of fluorophores did not improve the model fit, leading to poorly defined profiles for the extra components.

The obtained emission and excitation profiles for the three-component model (Figure 5A and B, respectively) are in good agreement with the expectations based on pure analyte standards. Furthermore, the kinetic analyte profiles (Figure 5C) are also coincident with those previously reported.^{44,45} In the case of urine, the emission and excitation profiles correspond to those known for unspiked urine samples, while the kinetic profile indicates that the major reaction in the presence of permanganate leads to degradation and slow fluorescence decay.

TLLS was then applied to the same set. In all samples, the study of the prediction residuals led to the conclusion that more than two components were required to improve the fit. Thus, to apply the RTL procedure, replication of blank samples was

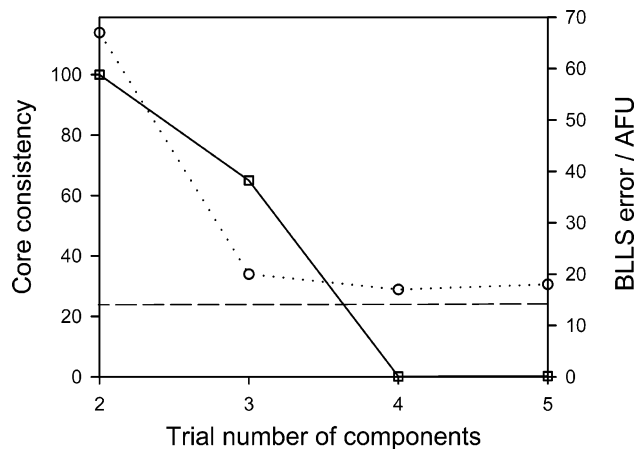


Figure 4. PARAFAC core consistency values (squares) and TLLS least-squares error (circles) as a function of the trial number of components for the analysis of the first spiked urine test sample of Table 2. The solid and dotted lines connecting the points (PARAFAC and TLLS, respectively) are a guide for the eye. The horizontal dashed line indicates the average instrumental noise level. AFU, arbitrary fluorescence units.

Table 2. Predicted Concentrations in Spiked and Blank Urine Samples Using Both PARAFAC and TLLS

nominal spiked	LV/mg L ⁻¹		MTX/mg L ⁻¹		
	PARAFAC	TLLS	nominal spiked	PARAFAC	TLLS
0.49	0.40	0.28	0.43	0.43	0.35
0.45	0.38	0.21	0.46	0.41	0.35
0.38	0.34	0.21	0.39	0.36	0.30
0.32	0.26	0.15	0.37	0.29	0.26
0.43	0.38	0.24	0.41	0.41	0.34
0.38	0.15	0.13	0.45	0.24	0.30
0.43	0.41	0.29	0.41	0.47	0.38
0.38	0.35	0.25	0.45	0.43	0.39
0.00	0.03	-0.05	0.00	-0.06	0.01
0.00	0.01	-0.05	0.00	-0.03	0.01
0.00	0.03	-0.04	0.00	-0.04	-0.01

figures of merit ^a	LV		MTX	
	PARAFAC	TLLS	PARAFAC	TLLS
RMSEP/mg L ⁻¹	0.10	0.17	0.08	0.08
SEN/AFU 1 mg ⁻¹	4 × 10 ³	4 × 10 ³	6 × 10 ³	6 × 10 ³
LOD/mg L ⁻¹	0.02	0.02	0.02	0.02

^a RMSEP, root-mean-square error of prediction. AFU, arbitrary fluorescence units. The value of SEN was computed using eq 14.

performed to obtain an average instrumental noise level of ~15 (arbitrary fluorescence units). Figure 4 shows that the TLLS error fit in the case of the first test sample of Table 2 stabilizes at three constituents, in agreement with the PARAFAC results. Furthermore, the spectral and time profiles provided by RTL for the urine background (Figure 5) are also similar to those furnished by PARAFAC. This result allows one to conclude that TLLS is successful in obtaining profiles for exploiting the second-order advantage.

Prediction results for the spiked urine set are presented in Table 2. All predictions are seen to be reasonable for samples of

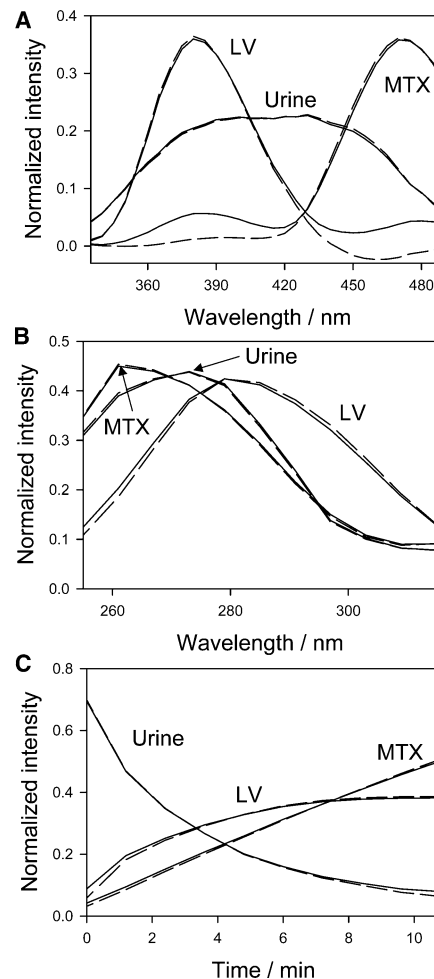


Figure 5. guideA) Fluorescence emission profiles, normalized to unit length, as found by PARAFAC (—) and by TLLS (---), after processing the first spiked urine test sample of Table 2. guideB) Excitation profiles. guideC) Kinetic time profiles. In all cases, the analyte profiles were identified by comparison with standards, with the remaining ones corresponding to the urine background (as indicated).

the complexity of human urine. Note that both algorithms are also successful in what concerns urine blanks, where analyte concentrations on the order of the limit of detection are found. The figures of merit are, however, poorer than for the binary test set described in the previous section. This is understandable on the basis of the increasing overlap in the three modes caused by the presence of urine components. The analyte concentration ranges have been chosen as representative of the expected ones in real samples; although they are somewhat narrow, they allow for estimation of sensitivity and LOD as is standard practice in the multivariate literature.^{51–59} In comparing the root-mean-square errors of prediction values provided by both algorithms, it seems that PARAFAC performs somewhat better than TLLS in the case of MTX, but the overall prediction ability of both methods appears to be comparable. It should be noted that even when the figures of merit are of inferior quality to those obtained for the binary test set, the present methodology provides a simple means of modeling serious overlapping interferences not contained in the calibration set of samples. Systems of this type constitute a significant challenge for multivariate methods.

Method Comparison. Since direct methods such as GRAM or DTLTD cannot be used for analyzing four-way data, N-PLS, PARAFAC, and TLLS are left for this purpose. From these latter methodologies, only PARAFAC and TLLS are able to achieve the second-order advantage. These multiway chemometric methodologies might be compared on the basis of (1) analytical performance, (2) model interpretability, and (3) ease and speed of program operation. Both TLLS and PARAFAC are able to handle the occurrence of interferences not contained in the training sample set, a property of immense utility in the analytical context. They also yield multimode profiles of useful physical meaning, which for the presently studied example are in mutual pleasant agreement. As regards computer operation, the methods can be programmed in MATLAB and introduced into a friendly, user-interface mode, and hence, no significant differences can be established in this respect.

CONCLUSIONS

PARAFAC and TLLS as chemometric assisting techniques have been applied for the determination of methotrexate and leucovorin in human urine samples, despite the serious interference from the urine background components. This is possible thanks to the third-order advantage, achieved when using four-way kinetic–EEMs arrays, because the data allow for the determination of mixture components in very complex samples containing uncalibrated interferences.

Kinetic–spectrofluorometric methods of this kind require a strict time control. Because a commercially available spectrofluorometer is fast enough to allow the recording of the EEMs, in the excitation and emission ranges indicated, in a time as short as 12 s, data acquisition is possible in the time domain, easily generating the required four-way data arrays.

The use of four-way arrays of data, particularly exploiting the information contained in a full fluorescence EEM spectrum, in combination with kinetic methods and advanced third-order chemometric modeling methods, merits further investigation. We have provided a new algorithm, trilinear least squares, which can be employed in a complementary way to PARAFAC to explore the analytical characteristics of these higher-order data. Further work is required in order to fully understand the properties of the newly introduced algorithm, but the results presented here indicate that it is a promising alternative to existing chemometric tools.

ACKNOWLEDGMENT

Financial support from CONICET (Consejo Nacional de Investigaciones Científicas y Técnicas), Universidad Nacional de Rosario, Agencia Nacional de Promoción Científica y Tecnológica (Project PICT 99, 06-06078) and the Ministerio de Ciencia y Tecnología of Spain (Project BQU2002-00918) is acknowledged. J.A.A. thanks CONICET for a fellowship.

ACKNOWLEDGMENT

Received for review May 11, 2004. Accepted July 29, 2004.

AC0493065